J Nanopart Res (2009) 11:121–131
DOI 10.1007/s11051-008-9453-5

Dustiness test of nanopowders using a standard rotating drum with a modified sampling train

Chuen-Jinn Tsai · Chien-Hsien Wu · Ming-Long Leu · Sheng-Chieh Chen · Cheng-Yu Huang · Perng-Jy Tsai · Fu-Hsiang Ko

Received: 28 May 2008 / Accepted: 6 June 2008 / Published online: 2 July 2008

Abstract The standard rotating drum tester was used to determine the dustiness of two nanopowders, nano-TiO_2 and fine ZnO, in standard 1-min tests. Then, the sampling train was modified to determine the number and mass distributions of the generated particles in the respirable size range using a Scanning Mobility Particle Sizer (SMPS), an Aerodynamic Particle Sizer (APS) and a Multi-orifice Uniform Deposit Impactor (MOUDI) in the 30-min tests. It was found that very few particles below 100 nm were generated and the released rate of particles decreased with increasing rotation time for both nanopowders in the 30-min tests. Due to the fluffy structure of the released TiO_2 agglomerated particles, the mass distributions measured by the MOUDI showed large differences with those determined by the APS assuming the apparent bulk densities of the powders. The differences were small for the ZnO agglomerates, which were more compact than the TiO_2 agglomerates.

C.-J. Tsai (✉) · C.-H. Wu · M.-L. Leu · S.-C. Chen · C.-Y. Huang
Institute of Environmental Engineering, National Chiao Tung University, Hsinchu 300, Taiwan, ROC
e-mail: cjtsai@mail.nctu.edu.tw

P.-J. Tsai
Department of Environmental and Occupational Health, National Cheng Kung University, Tainan, Taiwan, ROC

F.-H. Ko
Institute of Nanotechnology, National Chiao Tung University, Hsinchu, Taiwan, ROC

Keywords Nanoparticle · Dustiness · Aerosol sampling · Aerosol instrument · Nanotechnology · Occupational health · EHS

Introduction

Excessive levels of dust emissions during the handling and transport processes of powder materials can cause adverse health effects on workers and may also pose fire explosion hazards. It is therefore important for industrial hygienists to understand the propensity or dustiness of powder materials for the purpose of risk assessment and control (Mark 2005; CEN 2006).

Different dustiness test methods have been developed to quantify the dustiness of powder materials, in which different test apparatus and particle characterization methods are used (Hamelmann and Schmidt 2003). Results are expressed in different ways and are not directly comparable, and some of them do not classify the generated dust into three health-related size fractions: inhalable, thoracic and respirable dusts. Recognizing the need to standardize the test and ensure reproducibility, the European standard EN 15051 (CEN 2006) was published, which specifies two reference test methods for dustiness testing: rotating drum and continuous drop methods. The rotating drum method is a frequently employed method due to its ability to simulate a wide range of material handling processes for the estimation of dustiness (Mark 2005; Petavratzi et al. 2007).

The rotating drum method is based on the British MDHS 81 method (Lidén 2006), in which the generated dust is sampled into three dustiness fractions and the dustiness of the material is classified into four categories based on the mass fractions in each health-related fraction. However, no detailed size distribution can be obtained from this method, especially in the nanoparticle size range, or particles below 100 nm in diameter. Nanotechnology is one of the rapidly growing industries and many new nanomaterials are produced yearly. There is a growing concern over the toxicity of nanomaterials as increasing numbers of worker are exposed to nanoparticles. Therefore, it is important to understand the dustiness of nanopowders as it is directly related to the exposure levels and hence the health risks during handling of nanopowders.

In order to determine the number distribution of emitted nanoparticles, additional particle sizing instruments have to be used. Mark et al. (2007) used a SMPS and an APS in their standard rotating drum tester to test the number distributions of nanoparticles. They found that nanoparticles generated in the rotating drum were agglomerates, and the concentration of nanoparticles was low. The above two real-time aerosol instruments were also used in the dust generation studies of Maynard et al. (2004) and Isamu et al. (2007), who used a vortex shaker for the tests. Maynard et al. (2004) tested two unrefined single-wall carbon nanotube (SWCNT) materials and found that the laser ablation SWCNT was too compacted to release aerosols, while the concentration of fine and nanosize particles released from the HiPCO SWCNT increased with the increasing agitation level. Isamu et al. (2007) tested SWCNTs, TiO_2 and ZnO nanopowders and found that the number median diameter (NMD) of the generated particles was greater than 100 nm. No obvious changes in the particle size distributions of aerosols were observed regardless of the level of agitation and the amount of test nanopowders used for the test. However, the total number concentration changed with the agitation time up to few hours.

Schneider and Jensen (2008) used a Fast Mobility Particle Sizer (FMPS, TSI Model 3091) and an APS (TSI model 3321) in their small rotating drum of 5.9 L, which is much smaller than the rotating drum of the EN 15051 standard. They found that the pigment-grade TiO_2 had the lowest dustiness, while the ultrafine TiO_2 had the highest dustiness as measured by particle number. Three types of time profiles of the dust generation rate were observed, including brief initial burst (talc and corundum), decaying rate during rotation period (fumed silica, TiO_2 ultrafine and pigment grade, and bentonite) and constant rate (Y-zirconia and goethite).

The above real-time instruments have been used widely. However, there are some problems reported with these instruments in the literature. For example, in the SMPS measurements, Ku et al. (2007) observed anomalous responses above certain voltages in the DMA when characterising aggregates of airborne carbon nanotubes or nanofibers. This anomalous behaviour was associated with a sudden increase in measured number concentration. Peters and Leith (2003) found that the counting efficiencies of the TSI model 3321 APS were low, which were about 20% for 0.52-, 45% for 2- and increased to 60% for 4-μm oil particles. These low counting efficiencies for oil particles led to lower measured mass concentration with the APS 3321 than that measured with the impactor. Volcken and Peters (2005) also found low counting efficiencies of the APS 3321 for liquid particles, but the counting efficiency for solid particles was found to be high, which ranged from 85 to 99% for particles from 0.8 to 10 μm in aerodynamic diameter. There are no counting efficiency data available for solid particles less than 0.8 μm, but the efficiencies are expected to be higher than those of liquid particles. Kinney and Pui (1995) reported particle losses of the APS due to superisokinetic sampling at the entrance of the inner inlet and from inertial impaction of particles on the surface of the inner nozzle.

The above real-time instruments measure particle number distributions only. However, the surface area of aerosols maybe more relevant to heath risks than other measurement metrics (Oberdörster et al. 2005). In addition, the recent recommended exposure limits of fine and nano-TiO_2, which are 1.5 and 0.1 mg/m^3, respectively, are expressed in terms of mass concentration (NIOSH 2005). It is therefore desirable to use additional particle instruments to gain additional and more accurate mass distribution data for the generated particles. In this study, the dustiness was measured based on the standard 1-min rotating drum method first. Then, additional 30-min tests using the SMPS (TSI model 3936), the APS (TSI model 3321)

and the MOUDI (MSP model 110) were conducted to obtain the number and mass distributions simultaneously of the generated dust after the two-stage porous foams but without the backup filter. The obtained dustiness data and number distributions were compared with the previous experimental data in the literature. The mass distributions obtained from the MOUDI were compared with the converted mass distributions from the SMPS and the APS assuming apparent bulk densities of the powders determined in this study. Densities which gave the same total mass concentrations compared to the MOUDI were also found for both TiO_2 and ZnO. Differences between the fitted bulk densities and the bulk densities of the powders were explained in the light of the different morphologies of the agglomerated particles observed under the SEM.

Experimental

In this study, Nano-TiO_2 (Degussa AEROXITE TiO_2 P25) and fine ZnO (Sun Beam, Grade A, Taiwan) powders were tested. The properties of the tested materials are given in Table 1, where the apparent bulk densities are 0.13 g/cm^3 for TiO_2 and 0.6 g/cm^3 for ZnO powders, as determined according to CEN 15051 in this study. These bulk density values are much lower than the corresponding densities of the bulk materials, which are 3.90 and 5.67 g/cm^3 for anatase TiO_2 and ZnO minerals, respectively. Dustiness tests were conducted based on the EN 15051 rotating drum test method for 1 min at the flow rate of 38 L/min. Instead of using a glass fiber filter, a HEPA filter was used in front of the drum to remove ambient particles. The test powders were dried in an oven controlled at 105 °C for at least 2 h prior to the tests.

The standard rotating drum dustiness tester used in this study is described in EN 15051 (CEN, 2006). It comprises a 300-mm diameter stainless steel drum rotating at 4 rpm, equipped with eight longitudinal vanes to lift and let fall a known volume (35 cm^3) of the material under test, and a three-stage dust sampling system through which the emitted dust cloud is drawn by a vacuum pump at a flow rate of 38 L/min for the duration of 1 min. The sampling system comprises two particle size-selective foam stages in series followed by a backup filter, which is a quartz filter. Dust entering the conical passage and into the sampling system gives an estimate of the inhalable fraction. The size selectors, in the form of cylindrical plugs of 20 ppi (pores per inch) and 80 ppi porous foams, are used to select the thoracic and the respirable fractions, respectively. The foams and the backup filter are weighed before and after the test to provide the dustiness estimates of the three size fractions.

After the dustiness tests, size distribution measurements were conducted, each lasting for 30 min on the rotating drum tester, as shown in Fig. 1. The sampling train was modified to consist of the

Table 1 Comparison of dustiness of TiO_2 and ZnO powders

	Crystallite size, nm	Dustiness mass fraction, mg kg^{-1}			
		Inhalable	Thoracic	Respirable	
TiO_2, Mark et al. (2007)[a]	150	610 (Low)	60 (Low)	20 (Low)	
TiO_2, Schneider and Jensen (2008)[b]	149.4	31 (Very low)	–	–	
	18.6	8338 (High)	–	–	
TiO_2, Present work[d,e]	21	6713 ± 546 (High)	576 ± 37 (Moderate)	15 ± 2 (Low)	8.32 ± 0.76[c] (Very low)
ZnO, Present work[d,e]	250–300	142 ± 20 (Very low)	72 ± 6 (Low)	11 ± 0.3 (Low)	2.33 ± 0.13[c] (Very low)

[a] EN15051 (CEN 2006)

[b] 5.9 L small rotating drum

[c] Measured by MOUDI and converted to 1-min equivalent mass fraction at 38 L/min

[d] Number of sample = 3

[e] Apparent bulk density = 0.13 g/cm^3 (TiO_2), 0.6 g/cm^3 (ZnO), determined according to CEN 15051

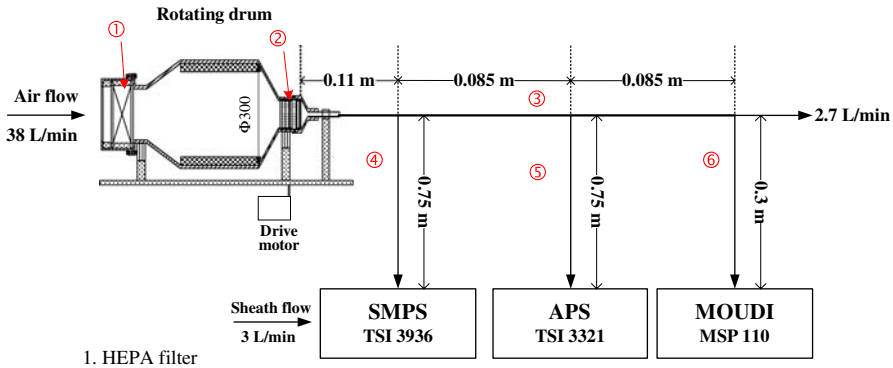

Fig. 1 Experimental setup of the standard rotating drum tester with the modified sampling train. The after filter was removed when the size distribution measurements were to be conducted

MOUDI, the SMPS and the APS without the backup filter but with the porous foams of the two stages in the sampling section. The two porous foam stages were used to remove particles greater than the respirable size for the size distribution tests. The penetration efficiency of nanoparticles of 20 to 100 nm in diameter for the two 1st stage 20 ppi foams and the 2nd stage 80 ppi foam were measured using polydisperse NaCl test aerosols and found to range from 88.2 to 97.8%, and 71.9 to 94.4%, respectively, at 38 L/min. These penetration data indicate that the size distribution measurements by the present sampling train in the respirable size range have a small bias. The sampling flow rate of the SMPS was set at 0.3 L/min with a sheath flow of 3 L/min (mobility diameter range: 15–650 nm), while those of the APS and MOUDI were 5 and 30 L/min, respectively. The SMPS and APS were used to monitor the background particle level until it was reduced below 1 #/cm^3 before a 30-min test started.

The aluminium foil substrates of the MOUDI were coated with silicon grease for about 3 mg to reduce particle bounce. The after filter of the MOUDI is a glass fiber filter. The foams and backup filter of the sampling train, and the substrates and the after filter of the MOUDI were stored for 24 h in a chamber controlled at a constant relative humidity condition of 40 ± 5%. The weight of the foams was measured using a Sartorius CP225D electrical microbalance (accuracy ± 20 μg) and that of the filters and coated aluminium foils were measured using a Sartorius CP2P-F electrical microbalance (accuracy ± 1 μg) at a constant temperature and relative humidity condition of 22 ± 0.4 °C and 40 ± 3%, respectively. The weight of each sample was measured at least five times to make sure the variation between measurements was within 4 μg for the filters and coated aluminium foils or 100 μg for the foams on the same day. The blank foams, filters and coated aluminium foils were weighed on different days to determine the day-to-day variations of weighing. Due to their ready absorption of water vapour, the standard deviations of the blank foams were found to be large, which were 503.1 μg for the two 20 ppi foams (nominal weight: 3,243 mg) with a thin plastic container (nominal weight: 8,755 mg) and 80.1 μg for the 80 ppi foam (nominal weight: 1,853 mg). These large standard deviations may present challenges for the nanopowders with small bulk density and very low dustiness index of inhalable and thoracic fractions. In comparison, the weighing of filters and aluminium substrates was much more accurate with the standard deviation of 25.3 μg for the backup quartz filter (nominal weight: 370 mg), 7.4 μg for the glass fiber filter (nominal weight: 58.4 mg) and 5.48 μg for the coated aluminium substrates (nominal weight: 71.9 mg).

When comparing the mass distributions of the MOUDI with those converted from the APS and the SMPS, the apparent bulk densities determined in this study were assumed. Densities which fitted the total mass concentrations of the MOUDI were also found for both TiO_2 and ZnO. In order to facilitate the comparison between the converted mass distributions and the MOUDI's mass distributions, SEM pictures were taken by a JSM-6701F (JEOL Ltd., Tokyo, Japan) field emission scanning electron microscope (FESEM)

under an accelerating voltage of 30 kV for the particles collected on the backup filters and the substrates of the MOUDI. Prior to SEM characterization, samples mounted on the SEM grids were coated with platinum metal to avoid the image charging problem.

Results and discussion

Dustiness of TiO_2 and ZnO powders, standard test

The result of the present dustiness test are shown in Table 1, where it shows the dustiness mass fractions for TiO_2 are 6713 ± 546, 576 ± 37and 15 ± 2 mg/kg^{-1}, which are classified as high, moderate and low dustiness for the inhalable, thoracic and respirable fractions, respectively, based on the 1-min standard test. The respirable dust fraction determined from the 30-min MOUDI test is about half of the standard 1-min test or 8.3 ± 0.76 mg/kg^{-1}. One possible reason is due to the decaying dust generation rate of the released dust during the rotation period, which will be discussed later. Different methods used to determine the respirable dust fraction could also be another reason leading to the differences. For the nano-TiO_2 powder, the present inhalable mass fraction is classified as high dustiness and is comparable to that obtained by Schneider and Jensen (2008), who used a small 5.9 L rotation drum for the test. In comparison, the data shown in Table 1 from Mark et al. (2007) and Schneider and Jensen (2008) all indicate that fine TiO_2 powders have low or very low dustiness for all three mass fractions.

The present dustiness test results for fine ZnO powder show that the dustiness mass fractions are 142 ± 20, 72 ± 6 and 11 ± 0.3 mg/kg^{-1}, classified as very low, low and low dustiness for the inhalable, thoracic and respirable dusts, respectively, based on the 1-min standard test. The respirable dust fraction determined from the 30-min MOUDI test is again much lower than that of the standard 1-min test or 2.3 ± 0.1 mg/kg^{-1}, possibly due to the decaying dust generation rate during the rotation period and the differences in the measurement methods.

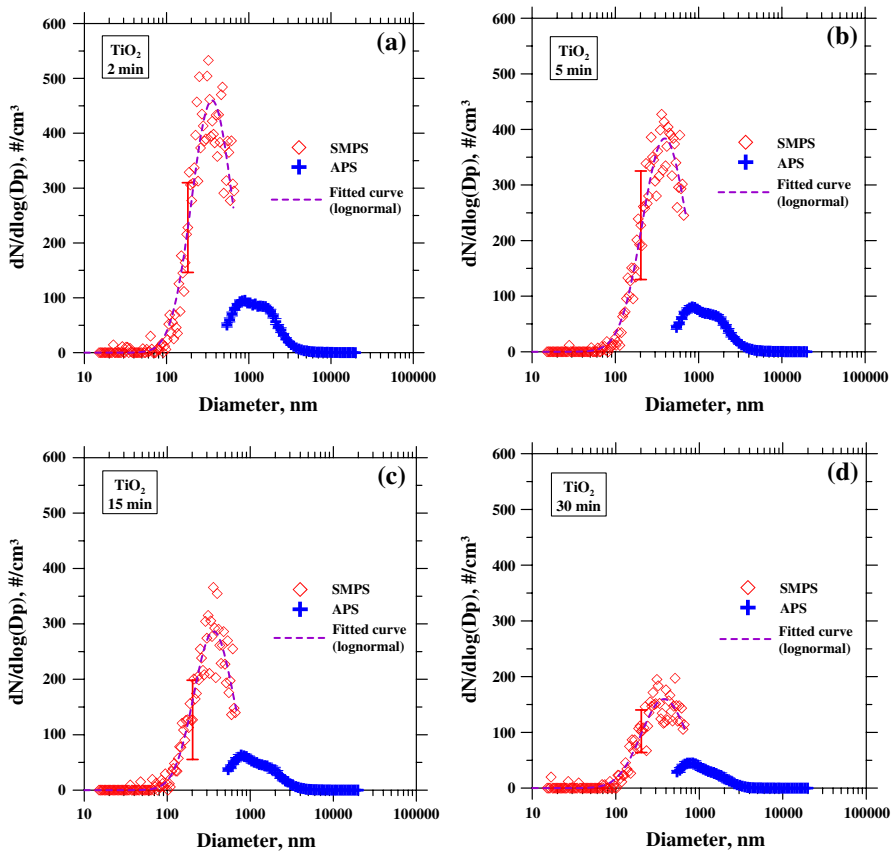

Fig. 2 Real time number distribution measurement, TiO_2 powder, 30-min test. A typical error bar is shown in the figure. Number of sample = 6, SMPS, electric mobility diameter; APS, aerodynamic diameter

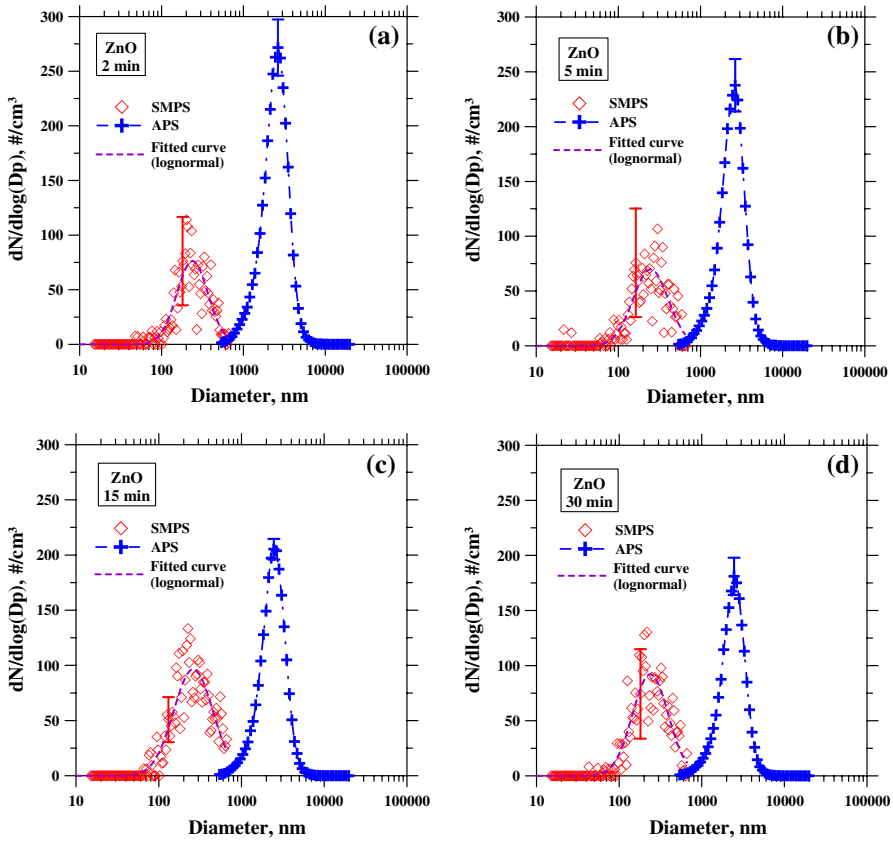

Fig. 3 Real time number distribution measurement, ZnO powder, 30-min test A typical error bar is shown in the figure. Number of sample = 6, SMPS, electric mobility diameter; APS, aerodynamic diameter

Real-time number distributions in the respirable size range

The real-time number distributions of the generated dust in the respirable size range are plotted in Figs. 2 and 3 for TiO_2 and ZnO powders, respectively, where the diameter of the SMPS and APS data is expressed in electrical mobility and aerodynamic diameter, respectively. It is to be noted that the APS data were not corrected for counting efficiency described in the "Introduction" section. Both figures show that during the 30-min test, nearly no particles below 100 nm in electric mobility diameter are generated from both powders, as measured by the SMPS. The average total particle concentrations below 100 nm are only 1.87 and 1.74 #/cm^3, which correspond to 7.84×10^{-5} (assuming TiO_2 bulk density is 0.13 g/cm^3) and 3.72×10^{-4} (assuming ZnO bulk density is 0.60 g/cm^3) μg/kg-min for TiO_2 and ZnO, respectively. During the 30-min test, 10 sets of 2-min SMPS and APS data were obtained for each powder and only the data at 2, 5, 15 and 30 min are shown. It can be seen that the number distribution of TiO_2 decreases from the peak value of 532.9 #/cm^3 at 2 min to 197.2 #/cm^3 at 30 min for the SMPS data, and 95.3 #/cm^3 at 2 min to 45.0 #/cm^3 at 30 min for the APS data (Fig. 2). The shape of the distribution function does not change very much with the NMD of 356 to 391 nm and the GSD of 1.7 to 1.88 for the SMPS data, and the NMAD (number median aerodynamic diameter) changes slightly from 898 to 835 nm for the APS data during the 30-min test.

For the fine ZnO powder, much lower particle concentration below 1,000 nm is generated compared to the TiO_2 powder and the SMPS data show that the number distributions remain to be similar with the peak value of 107 to 144 #/cm^3, NMD of 239 to 261 nm, and GSD of 1.55 to 1.73 during the 30-min test. Compared to TiO_2, there are more particles detected by the APS, and the peak number concentration is decreased from 271.7 #/cm^3 at 2 min to 181.1 #/cm^3 at 30 min, while the NMAD changes slightly from 2,642 nm to 2,458 nm during the 30-min test.

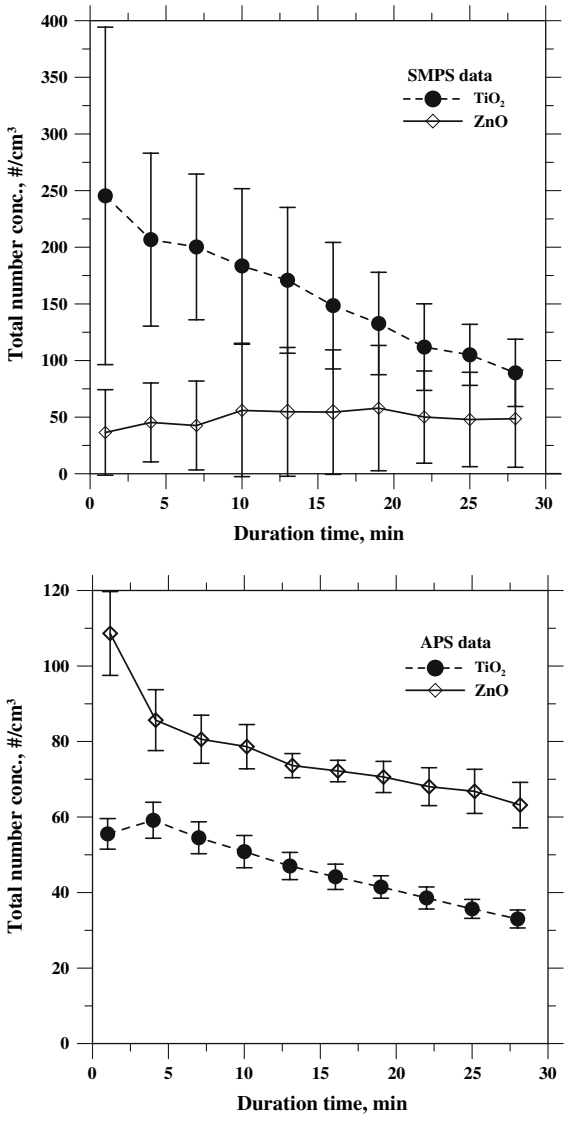

Fig. 4 Total particle number concentration with rotation time, 30-min test

The decaying total particle concentrations versus rotation time during the 30-min test are plotted in Fig. 4 for both powders. All except the SMPS data for ZnO show clear decaying trend with the rotation time. The total concentration of submicron ZnO particles is low and varies between 0 and 100 #/cm^3 with the rotation time. By using the FMPS, Schneider and Jensen (2008) also showed that the dust generation decayed during the 1-min rotation time for fumed silica, TiO_2 ultrafine and pigment grade and bentonite, but remained constant for Y-zirconia and goethite. The decaying particle generation observed

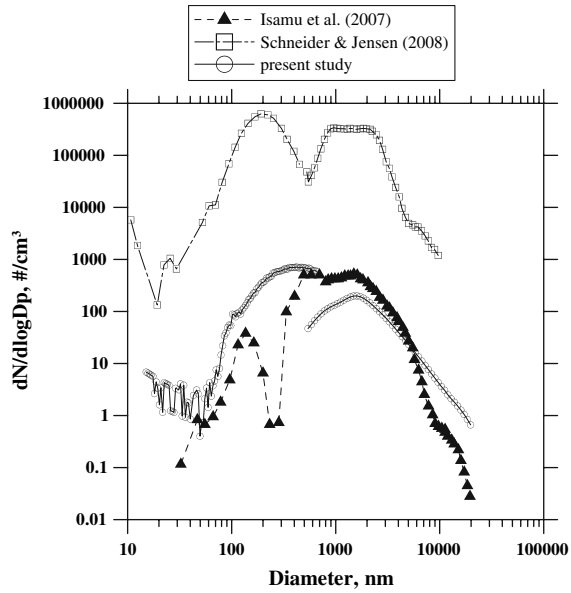

Fig. 5 Comparison of the present 30-min average real-time size distributions of the generated particles with those of the previous investigators

in the APS data also explains why the respirable dust concentration determined from the 30-min sampling time of MOUDI is much lower than that determined in the 1-min standard test shown in Table 1.

For comparison purpose, there are real-time size distribution data in the literature for nano-TiO_2 obtained by Isamu et al. (2007) using a vortex shaker and by Schneider and Jensen (2008) using a small rotation drum of 5.9 L, which is much smaller than the standard drum volume of 22.3 L. Comparison of the present 30-min average real-time size distributions of the generated particles with those of the previous investigators is shown in Fig. 5 and the test parameters used in the present study and the previous two investigators are shown in Table 2. All three test data show similar bimodal distribution. The NMD in the submicron size range of the present study is about 300 nm, which is larger than the previous two studies (140–200 nm), while the NMAD of the supermicron size range are similar and fall between 1 and 2 μm. Although the test methods and nano-TiO_2 are different, it is seen that the present average number distribution in 30 min is similar to the average distribution (170–205 min after agitation started) of Isamu et al. (2007) who used a vortex shaker with only 0.25 cm^3 of nano-TiO_2 for the test compared with the present 35 cm^3 (or 4.5 g). While it is not

Table 2 Comparison of the present real time test parameters with previous studies, TiO_2 powder

	Present work	Schneider and Jensen (2008)	Isamu et al. (2007)
Method	Rotating drum	Rotating drum	Vortex shaker
Particle sizer	SMPS, APS	FMPS, APS	SMPS, APS
TiO_2 nanopowder manufacturer and model	Degussa, P25	Kemira UV-TITAN M111	Ishihara Sangyo Kaisha, ST-01
Primary particle size	21 nm	18.6 nm	~7 nm
Sample amount	35 cm^3 (4.5 g)	6 g	0.25, 0.5, 1.0 cm^3
Total flow rate	38 L/min	11 L/min	5 L/min
Lifter vanes	8	3	–
Sampling time	2 min[a]	1 s	5 min
Rotation speed	4 rpm	11 rpm	–
Chamber volume	22.3 L	5.9 L	0.1 L

[a] Average of ten 2-min sampling data during 30-min test

clear whether the agreement is fortuitous, both number distribution functions are much lower than that of Schneider and Jensen (2008) who used a small rotating drum and 6 g of nano-TiO_2 in the test. The major difference is that Schneider and Jensen (2008) used a TSI FMPS and a TSI APS at 1-s sampling period in the 1-min tests, which was able to detect the brief initial burst and dust generation at a very early stage of the test, while each SMPS data in the present study and Isamu et al. (2007) took 2 and 5 min, respectively, for obtaining a distribution data and the test lasted for 30 min and longer.

Comparing the mass distribution of MOUDI, APS and SMPS in the respirable size range

In addition to the number distribution data, additional mass distribution data were obtained by the MOUDI in the 30-min test in the respirable size range. The results of TiO_2 and ZnO are plotted in Fig. 6 together with the converted mass distribution data from the SMPS and APS. It is seen that the mass median aerodynamic diameters (MMADs) of both powders fall between 3.2 and 5.6 μm, which is the size range of the 3rd stage of the MOUDI. This is to be expected since only respirable particles were sampled by the MOUDI and monitored by the other two real-time instruments. The fitted mass distribution function (not shown in the figures) using the TSI Disfit program gives an MMAD of 4.45 and 4.01 μm, and GSD (geometric standard distribution) of 1.83 and 1.67, for TiO_2 and ZnO, respectively. The total respirable mass fractions obtained from the 30-min and 30-L/min MOUDI test are 197 ± 18 and 55.2 ± 3.1 mg/kg, for TiO_2 and ZnO, respectively. When converted to the equivalent mass fractions of the 1-min standard dustiness test at 38 L/min, they become 8.32 ± 0.76 and 2.33 ± 0.13 mg/kg, as shown in Table 1. These respirable mass fractions are much smaller than those of the standard test due to the decaying dust generation with the rotation time as explained earlier.

The mass concentrations of nanoparticles were obtained by the MOUDI and were converted to the equivalent nanoparticle mass fraction of the 1-min standard dustiness test at 38 L/min. The nanoparticle mass fractions are 0.0136 and 0.0069 mg/kg for TiO_2 and ZnO, respectively. These values are below the detection limits of the MOUDI set by the weighing accuracy: 0.041 and 0.009 mg/kg for TiO_2 and ZnO, respectively. Therefore, the MOUDI data show that nanoparticle emission from the nanoscale and fine powders are negligibly low, which confirms the nearly zero nanoparticle mass concentrations converted from SMPS data shown in the figures.

The number distribution data of the SMPS and APS were converted to the mass distribution data using the bulk density of 0.13 and 0.6 g/cm^3 for TiO_2 and ZnO, respectively, determined in this study according to CEN 15051. The converted mass distributions from the SMPS show nearly zero concentrations for particles <100 nm, while those of the APS are shifted to the left of the MOUDI data with smaller MMADs. The shift is due to the fact that bulk densities of the nanoparticles are less than 1.0 g/cm^3 leading to underestimation of the aerodynamic

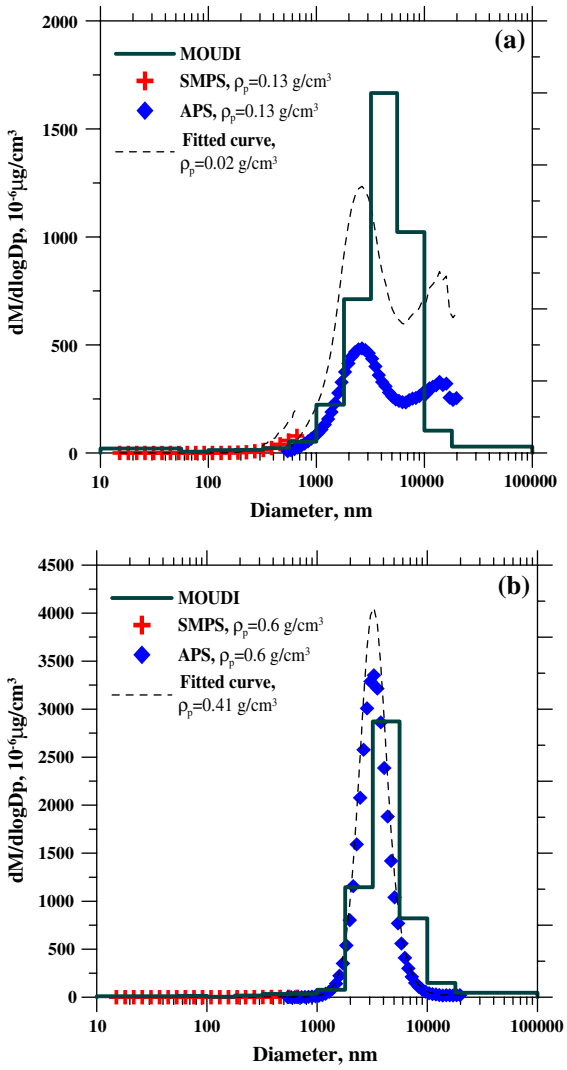

Fig. 6 Comparison of mass distributions of MOUDI with those converted from SMPS and APS. (**a**) TiO_2 (**b**) ZnO

diameter (Tsai et al. 2004). In the conversion of the SMPS and APS data, the assumption that particles are spherical may introduce errors and also contribute to the shift of the converted mass distribution of the APS. The shift could also be caused by the deformation of the agglomerated particles when they pass through the jet region of the APS and appear as smaller aerodynamic diameter (Baron 1986; Tsai et al. 1998). The converted mass distribution of nano-TiO_2 is much lower than the MOUDI with the peak concentration of the former of only 0.3 times of the latter. In comparison, the converted mass distribution of fine ZnO is much closer to the MOUDI with a similar peak concentration. Based on the same total mass concentration, the fitted curve shown in Fig. 6 gives an estimated bulk density of 0.02 and 0.41 g/cm^3 for TiO_2 and ZnO, respectively, which are smaller than that determined in this study, especially for TiO_2. For ZnO particles, the estimated bulk density of 0.41 g/cm^3 is closer to the value determined in this study, 0.6 g/cm^3, compared to TiO_2 particles. The large differences of the measured and estimated bulk densities for TiO_2 particles are due to their much larger geometric diameter compared to the aerodynamic diameter, which leads to a larger particle loss in the inner nozzle of the APS (Kinney and Pui 1995). Besides, Tsai et al. (1999) found the transmission efficiency through the nozzle of a similar aerodynamic sizer, called Aerosizer, was low. The larger fluffier TiO_2 particles will also have a smaller transmission efficiency than the more compact ZnO particles.

The above observations are supported by the SEM pictures shown in Fig. 7a for TiO_2 and b for ZnO particles on the quartz filters of the sampling train. It can be seen that agglomerated TiO_2 particles have a fluffy structure, while agglomerated ZnO particles are more compact. It is expected that the bulk density of the agglomerated TiO_2 and ZnO particles will be smaller than the bulk density of the corresponding powder, and the difference will be larger for TiO_2 particles, as discussed in this section.

Conclusions

This study is aimed at studying the dustiness as well as the average size distributions of nanopowders in the respirable size range using the standard rotating drum tester. The sampling train was modified to accommodate the number and mass distribution measurements by using the SMPS, APS and MOUDI and the test lasted for 30 min. In the modified sampling train, the porous foams of the two porous foam stages were remained in place, while the backup quartz filter was removed.

In the 1-min standard dustiness test, the porous foam was found to absorb water vapour readily leading to great challenges when nanopowders of very low dustiness were tested. It was found that the dustiness index obtained in this study for the nano-TiO_2 powder was comparable to that of the previous

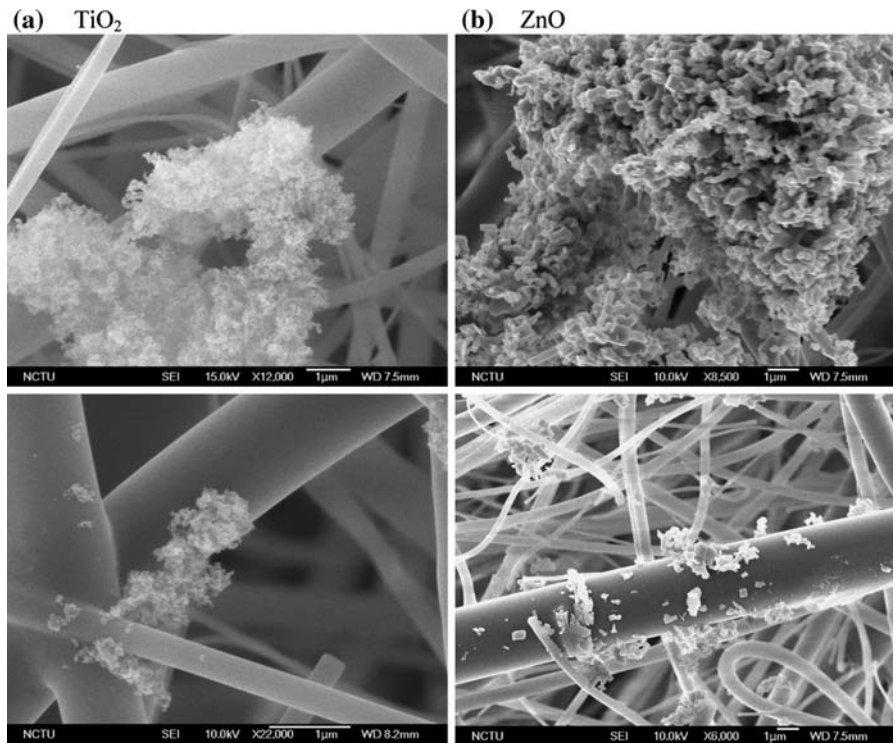

Fig. 7 SEM pictures. (**a**) TiO_2 (**b**) ZnO

investigators, the dustiness of which was higher than the ZnO powder of larger primary diameter. Using real-time sizing instruments, it was found that very few particles below 100 nm were released from these two nanopowders and the concentration of the generated submicron particles was higher for the TiO_2 than the ZnO powder. Decaying generation rate of particles with increasing rotation time was observed for both nanopowders in the 30-min tests. This leads to a smaller respirable mass fractions calculated from the MOUDI compared to that from the standard 1-min test. The mass distributions determined by the MOUDI were compared with the converted mass distributions from the number distributions of the APS and SMPS using the bulk densities of the nanopowders, and large differences were found for the TiO_2 powder. However, the differences were smaller for the more compact ZnO powder. This is due to the fluffier structure of the TiO_2 agglomerates compared to the more compact ZnO agglomerates, as observed in the SEM images of the generated particles.

Although the real-time instruments such as APS are convenient, this study shows that the size distribution measurements may not be accurate due to the fluffy morphologies of the released particles in the test. Therefore, it is recommend to test the particle release of more nanopowders using both manual methods and real-time instruments in the future.

Acknowledgement The financial support from the Taiwan National Science Council via the contract NSC 96-2120-M-006-005 is gratefully acknowledged.

References

Baron P (1986) Calibration and use of the aerodynamic particle sizer (APS 3300). Aerosol Sci Technol 5:55–67. doi: 10.1080/02786828608959076

CEN (European Committee for Standardization) (2006) Workplace atmospheres—Measurement of the dustiness of bulk material—Requirements and reference test methods. EN 15051:2006 (E) April 2006

Hamelmann F, Schmidt E (2003) Method of estimating the dustiness of indurstrial powders—A review. KONA—Powder Science & Technology in Japan No.21

Isamu O, Sakurai H, Gamo M (2007) Dustiness testing of engineered nano-materials. In: Abstract, 3rd international symposium on nanotechnology, occupation and environmental health, Taipei, Taiwan, 29 Aug–1 Sep 2007

Kinney PD, Pui DYH (1995) Inlet efficiency study for the TSI aerodynamic particle sizer. Part Part Syst Charact 12:188–193. doi:10.1002/ppsc.19950120405

Ku BK, Maynard AD, Baron PA, Deye GJ (2007) Observation and measurement of anomalous responses in a differential mobility analyzer caused by ultrafine fibrous carbon aerosols. J Electrost 65:542–548. doi:10.1016/j.elstat.2006.10.012

Lidén G (2006) Dustiness testing of materials handled at workplaces. Ann Occup Hyg 50(5):437–439. doi:10.1093/annhyg/mel042

Maynard AD, Baron PA, Foley M, Shvedova AA, Kisin ER, Castranova V (2004) Exposure to carbon nanotube material: aerosol release during the handling of unrefined single-walled carbon nanotube material. J Toxicol Environ Health Part A 67:87–107. doi:10.1080/15287390490253688

Mark D (2005) The use of reliable measurements of dustiness of chemicals in selecting the most appropriate dust control technology. IOHA 2005 Pilanesberg:S2-3

Mark D, Bard D, Thorpe A, Wake D (2007) Some considerations for the measurement of the dustiness of nanopowders. In: 3rd international symposium on nanotechnology, occupational and environmental health, Taipei, Taiwan, 29 Aug–1 Sep 2007

NIOSH (2005) NIOSH current intelligence bulletin: evaluation of health hazard and recommendations for occupational exposure to titanium dioxide (draft)

Oberdörster G, Oberdörster E, Oberdörster J (2005) Nanotoxicology: an emerging discipline evolving from studies of ultrafine particles. Environ Health Perspect 113:823–839

Petavratzi E, Kingman SW, Lowndes IS (2007) Assessment of the dustiness and the dust liberation mechanisms of limestone quarry operations. Chem Eng Process 46:1412–1423. doi:10.1016/j.cep. 2006.11.005

Peters TM, Leith D (2003) Concentration measurement and counting efficiency of the aerodynamic particle sizer 3321. J Aerosol Sci 34:627–634. doi:10.1016/S0021-8502(03)00030-2

Schneider T, Jensen KA (2008) Combined single-drop and rotating drum dustiness test of fine to nanosize powders using a small drum. Ann Occup Hyg 52(1):23–34. doi:10.1093/annhyg/mem059

Tsai CJ, Chein HM, Chang ST, Yoh KuoJong (1998) Performance evaluation of an API Aerosizer. J Aerosol Sci 29:839–853. doi:10.1016/S0021-8502(97)00433-3

Tsai CJ, Yang WS, Szymanski WW, Chein HM (1999) Particle transmission efficiency through the nozzle of the API aerosizer. J Aerosol Sci 30:1019–1028. doi:10.1016/S0021-8502(98)00789-7

Tsai CJ, Chen SC, Huang CH, Chen DR (2004) A universal calibration curve for the TSI aerodynamic particle sizer. Aerosol Sci Technol 38:467–474. doi:10.1080/02786820490460725

Volckens J, Peters TM (2005) Counting and particle transmission efficiency of the aerodynamic particle sizer. J Aerosol Sci 36:1400–1408. doi:10.1016/j.jaerosci.2005.03.009